Astron. Astrophys. 323, 71–85 (1997)

ASTRONOMY
AND
ASTROPHYSICS

Line spectra of Liners. The contribution of the different ionization mechanisms⋆

M. Contini

School of Physics and Astronomy, Raymond and Beverly Sackler Faculty of Exact Sciences, Tel-Aviv University, Ramat-Aviv, 69978 Tel-Aviv, Israel

Received 1 April 1996 / Accepted 15 November 1996

Abstract. The physical conditions which characterize individual Liners are obtained by fitting the observational spectra of the Ho et al. (1993) sample by model calculations. Composite models which consistently account both for shocks, accompanying the radial outward motion of the gaseous clouds, and a photoionizing radiation flux are used. Power-law or black body radiation is considered, depending on the characteristics of the line spectra. The SUMA code is used. The contributions of the different ionization mechanisms to the spectrum emitted by each object are calculated and compared with the observations.

The most significant line ratios of Liner spectra are analyzed to show the relative importance of photoionization by radiation from the active center or from starbursts, of photoionization by diffuse radiation, and of collisional ionization by shocks.

Model results show that [Ne V] lines can be strong due to collisional ionization and/or photoionization. Lines from the II and III ionization levels are usually due to photoionization, but a strong contribution by collisional ionization appears in case of high densities and/or of a strong shock. Neutral lines are enhanced by diffuse radiation. The contribution of high density gas to the line intensities in Liner spectra is very small, indicating that the high density region, located between the NLR and the BLR, is also small.

The results show that shocks play an important role, even if a photoionizing flux is present. On average, higher than cosmic N/H and lower S/H are indicated. The physical characteristics of Seyfert galaxies and of starburst galaxies are confirmed.

The satisfactory results obtained interpreting the heterogeneous observational sample by SUMA strengthen the hypothesis that shock signature in AGN spectra is due to cloud motions in galaxies.

Key words: galaxies: active – galaxies: starburst – galaxies: Seyfert – radiation mechanisms: nonthermal – shock waves

⋆ Tables 1 and 2 are only available in electronic form at CDS via anonymous ftp (130.79.128.5) or via http://cds web.u-strasb.fr/Abstract.html

1. Introduction

Liners (Low Ionization Nuclear Emission-line Region) are generally classified among active galactic nuclei (AGN). In fact, some of their spectra show the characteristic broad line component of the Balmer lines, and in a few objects a central UV source is observed. Liners, if identified with AGN objects, are located in the low luminosity tail of the AGN luminosity distribution. However, the line intensity ratios and the line profiles typical of Liner spectra differ from characteristic AGN spectra. In fact, some of these ratios and profiles are rather similar to those emitted from supernova remnants (SNR), and also from starburst galaxies (SB). Indeed, a correlation between AGN and SB is possible (Lonsdale et al. 1992; Terlevich et al. 1992) and the direct stimulation of one phenomenon by the other has been analyzed. For example, triggering of molecular clouds, collapse and star formation by shock waves or other influence from the AGN, and fuelling of the AGN accretion by mass injection into the interstellar medium from SB, mass loosing giants and supernovae (SN) are possible links between SB and AGN phenomena.

Shocks will be seen in SB as well as AGN. SN and SNR cause shocks from the ejected matter or by blast waves accelerating preexisting interstellar clouds. SNR show a large range of different spectra, and it is unrealistic to directly compare a single or averaged SNR spectrum with those of Liners. In fact, observed Liner spectra disagree in some line ratios with those calculated for SNR conditions. Shocks were, therefore, often dismissed as factors in the spectra. On the other hand, shock models consistent with AGN conditions show that this mechanism is important (Morse et al 1996).

Outflow of matter accompanies jets in extended radio lobes of AGN (Balik & Heckman 1983) creating shocks. Shocks in AGN arize not only in the large scale jets and winds outflows, but they also accompany the propagation of gaseous clouds in the narrow line emission region (NLR). However, radiation cannot be neglected in any galaxy, whether power-law flux from an AGN or black body radiation from a starburst. Very hot stars, as in hot planetary nebulae, were suggested to provide the ionization continuum in Seyfert 2 (Shuder & Osterbrock 1981, etc.) and Terlevich & Melnick (1985) claim that Liners are ionized by

star clusters old enough to contain massive stars with high temperatures equal or even greater than those of the hottest known nuclei of planetary nebulae. Bare core of W-R stars can reach temperatures up to 2 10^5 K. Terlevich et al (1992), moreover, suggest that very hot condensations created by shocks in SNR are strongly radiative and provide the source of black body radiation in the NLR clouds.

It has been shown (e.g. Viegas-Aldrovandi & Contini 1989, and Contini & Viegas 1992; Contini et al. 1995) that shocks coupled with photoionization can explain the very high and very low ionization lines emitted from the NLR of QSO and Seyfert galaxies (Sy), and that they are essential to the calculation of Liners spectra (cf Dopita & Sutherland 1995, 1996). Therefore, in this work we include both shocks and photoionization.

The observational sample by Ho et al. (1993) provides the spectra of 18 objects which fit the definition of Liners: [O II] 3727+ stronger than [O III] 5007, [O I] 6300 at least 1/3 as strong as [O III] 5007 (Heckman 1980), [O III] $>$ 3 Hβ and [N II], [O I], and [S II] stronger than Hα (Veilleux & Osterbrock 1987). Moreover, [O III] 5007+4959/[O III] 4363 is 18-22 (Lipari et al. 1993) and the [S III] 9532/Hα line ratio constitutes a powerful diagnostic to distinguish between shock and photoionization mechanism in Liners (Diaz et al. 1985).

Interestingly, the sample is heterogeneous: some of the included objects were formerly classified as SB, Sy 2, H II regions, etc. Actually, the same criterion which was adopted by Ho et al in the choice of the sample is adopted in the interpretation of the spectra throughout the present investigation. In fact, the ranges of the input parameters in the calculation process are chosen in agreement with the characteristic of Liners relative to the other AGN (Veilleux & Osterbrock 1987; Osterbrock et al. 1992, etc.): in particular, a lower photoionizing radiation flux from the active center, lower velocities corresponding to much narrow FWHM of the line profiles, lower densities of the emitting gas indicated by the presence of forbidden lines with low critical density for deexcitation (e.g. [N I] 5200). Notice, however, that also starburst galaxies are intrinsically fainter objects, and show narrower low ionization emission lines (Dahari & De Robertis 1988).

The observational sample provide spectra in the optical-near IR range. Most of the lines are emitted by forbidden transitions and are characterized by a low critical density for deexcitation of the emitting gas. These lines are emitted in the NLR of AGN. The spectra are rich in number of lines from various elements in different ionization stages. In particular, lines from relatively high ionization levels ([Ne V]) and neutral lines ([O I], [N I]) appear in the spectra. The large range of ionization levels constrains the modelling even if the observed frequency range is limited to the optic-near IR.

We treat Liners as we have done in previous works on AGN (Viegas & Contini 1994 and references therein), with a model of gas clouds moving radially outward in the NLR. A shock front forms on the outer edge of the clouds, while radiation hits the opposite (internal) edge, if the source is an active nucleus, or either the inner or outer edge if the radiation is thermal.

First, the main ionization processes are discussed: photoionization by the active center of the galaxy, ionization by starbursts, ionization by diffuse radiation, and collisional ionization by shocks. Then, calculated spectra are compared with the observational data. The SUMA code (Viegas & Contini 1994 and references therein) is used for the calculations. We are now able to investigate the nature of Liners by fitting the observed spectra, using either a power-law (pl) or a black body (bb) for the ionizing radiation.

The recent generation of photoionization models considers the multi-zone behavior of emission-line regions (e.g. Baldwin et al 1996) because single-zone photoionization models are inadequate to describe the emission line regions in AGN. Composite models which account $consistently$ for both shocks and photoionization are a valid alternative for the NLR. In fact, due to compression, the gas downstream is characterized by regions of very different densities and temperatures (cf Viegas & Contini 1994; Contini & Aldrovandi 1983, etc). The multi-zone model in this case is thus consistent with compression. Recently, models which considered a distribution on densities, velocities, and intensities of radiation from the active center on larger scales were successfully adopted in the fitting process of calculated to observed spectra of AGN (Contini & Viegas-Aldrovandi 1989; Contini & Viegas 1991). However, the ranges of the physical conditions deduced from line ratios in Liners confirm that they are consistent with those calculated in the low density-velocity-radiation intensity tail of the distribution. In particular, the spectra show the characteristic line ratios of Seyfert 2 galaxies or of Liners, depending on the intensity of the radiation flux.

Dense matter, which could contribute to the spectrum of some galaxies, is generally related to relatively broad line profiles of characteristic lines, indicating high velocities of the emitting gas (e.g. NGC 7213, Filippenko & Halpern, 1984). These cases link Liners and Seyfert 1 galaxies through a broad line emission region (BLR). The contribution to the line intensities by high density gas is discussed with particular care.

Finally, recent model calculations have been compared with Liner spectra in a general way (Contini & Viegas 1992; Ho et al. 1993, etc.); in this paper we try to fit the whole line spectrum for each individual object. A perfect fitting of the observational data by model calculations is senseless and the disagreement of particular line ratios indicates that in some objects various regions characterized by different physical conditions and different ionizing and heating mechanisms should be considered. Radiation from the active center and thermal radiation from stars and/or hot regions may ionize and heat different gaseous clouds in the same object with comparable importance. In this investigation we refer to the different ionization mechanisms and different contributions are calculated for each object.

In Sect. 2 the models are presented. Ionization processes are discussed and theoretical line ratios are given in Sect. 3. The contribution of high density gas is considered in Sect 4. Calculated line ratios are compared with the observations and the results are discussed for individual Liners in Sect. 5. Conclusions appear in Sect. 6.

2. The models

In composite models, such as those calculated by the SUMA code, the shock and the photoionizing radiation flux are consistently accounted for. A full description of SUMA is given in Viegas & Contini (1994 and references therein). Radiation from the active center (AC) is characterized by the power-law flux $F_\nu \propto \nu^{-\alpha}$ with intensity F at 1 rydberg (in units of photons $cm^{-2}\,s^{-1}\,eV^{-1}$), the spectral index, α, and the high-energy cutoff, E_c.

In the SB case the model is determined by the star temperature, T_*, and by the ionization parameter, U. Radiation has an exponential spectral distribution.

The other basic input parameters are the shock velocity, V_s, the preshock density, n_0, and the preshock magnetic field, B_0. H, He, C, N, O, Ne, Mg, Si, S, Cl, A, and Fe lines are calculated up to the 10th ionization level. Relative abundances come from Allen (1983).

Usually an outward motion of the clouds is considered, so the radiation from the active center reaches the inner edge of the clouds, opposite to the shock front edge. However, in the analysis of the ionization processes (Sect.3) we adopted a model such that the shock and the photoionization act on the same edge of the cloud, in order to compare more straightforwardly the different processes.

The gas entering the shock front is thermalized and a zone of high temperature is present downstream, close to the shock front. The temperature of the ions is $T_i \simeq 1.5 \times 10^5 (V_s/100\,km\,s^{-1})^2$ K. The characteristic densities of the NLR clouds ($\simeq 1000\,cm^{-3}$) are high enough to provoke rapid energy equipartition between ions and electrons, so the electron temperature $T_e = T_i$.

The calculations across a cloud are performed through plane parallel slabs of gas. In each slab the temperature, the density, and the fractional abundance of the ions are calculated. The geometrical thickness of each slab is iteratively calculated so as to permit smooth profiles of the physical parameters throughout a cloud which has a geometrical thickness of ~ 10 pc.

The geometrical thickness of the hot zone depends on V_s , because the higher $T_e$the lower the recombination coefficients of the ionized elements. It depends also on the density, because the higher the density, the higher the cooling rate of the gas. When the temperature reaches $\leq 10^5$ K the cooling rate increases due to strong line emission and strong compression; the temperature rapidly drops and the gas recombines. Diffuse radiation from the hot gas maintains the gas at $\leq 10^4$ K and low ionization lines are emitted.

Radiation can be very weak and even absent in some situations. In this case there will be a large zone of cold gas which emits the neutral lines. As the line strengths depend not only on the physical parameters, but also on the volume of gas emitting them, the neutral lines are strong.

The models presented in Table 1 are those which better fit Liner spectra. M0 is a shock dominated model (F = 0). M1 represents a model with low shock velocity, V_s , low preshock density, n_0, and low photoionizaing flux, F. M2 and M3 show still low V_s and low n_0, but a relatively higher F, so that photoionization should prevail on shocks. M4 shows the effect of a low high-energy cutoff. M5 is characterized by higher V_s and n_0 which are higher limits deduced by observations of Liners spectra. In this case the effect of the shock is strong because the gas is heated up to temperatures $> 10^6$ K. Also the densities are higher both due to a higher n_0 and to compression. $M1_d$ and $M3_d$ are characteristic of higher density. M6 and M7 represent SB models.

Line intensities relative to Hβ, the Hβ flux at the nebula, and the most indicative line ratios are given in Table 1 for the different models. The parameters which characterize the models are presented in the last rows of Table 1. For all models $B_0 = 10^{-4}$ gauss can be adopted following previous investigations (Contini & Aldrovandi 1986). A spectral index $\alpha = 1.5$ is adopted. It is well known that a single spectral index is inadequate to fit the observed spectral energy distribution (SED) of the continuum in AGN. However, the line ratios in the optical range calculated as functions of the spectral index show small variations in the range $1 \leq \alpha \leq 2$, if the photoionizing flux and the shock velocity are relatively low (cf. Contini & Aldrovandi 1983, Fig. 2). Moreover, it is difficult to deduce the spectral index of the photoionizing flux from the observed continuum at frequencies lower than those corresponding to the UV - X-ray range, because the SED represents the sum of bremmstrahlung radiations emitted by many slabs of gas in very different physical conditions (Contini & Viegas-Aldrovandi 1990, Fig. 2c).

The distribution of the temperature (solid lines) and of the density (dashed lines) across the cloud are given in the top region of Figs. 1 as functions of the distance from the shock front for most of the models presented in Table 1. The shockfront is on the left and is also reached by the photoionizing radiation. In the bottom of Figs. 1 the fractional abundances Ne^{+4}/Ne, O^{+2}/O, N^{+1}/N, N^{+0}/N (solid lines), and H^+/H (dashed lines) are shown (cf. Sect. 3). The temperature and density profiles downstream are determined by the postshock compression which affects the cooling rates. The maximum of the temperature downstream occurs in the gas when hydrogen becomes neutral. The increase in $T_e$at this point is due to the sudden decrease in the density of free electrons, whose inelastic collisions with the heavy elements provide the main source of cooling of the gas (Williams 1967).

3. The comparison of the ionization processes

The mechanisms responsible for ionization and heating of the gas in Liners are controversial. Photoionization by radiation from the AC, as in AGN, is generally assumed, however, photoionization by stars and previously heated gas may also be an important factor. Photoionization enhances the intensities of lines from intermediate ionization levels. Shocks can heat the emitting gas to higher temperatures, so that lines from very high levels are strong and X-rays are emitted. Neutral lines are generally strong in Liners. They are characteristic of SNR spectra in which the shock mechanism prevails. Since they are not emitted by hot gas, nor by gas ionized by a radiation flux, the strength of

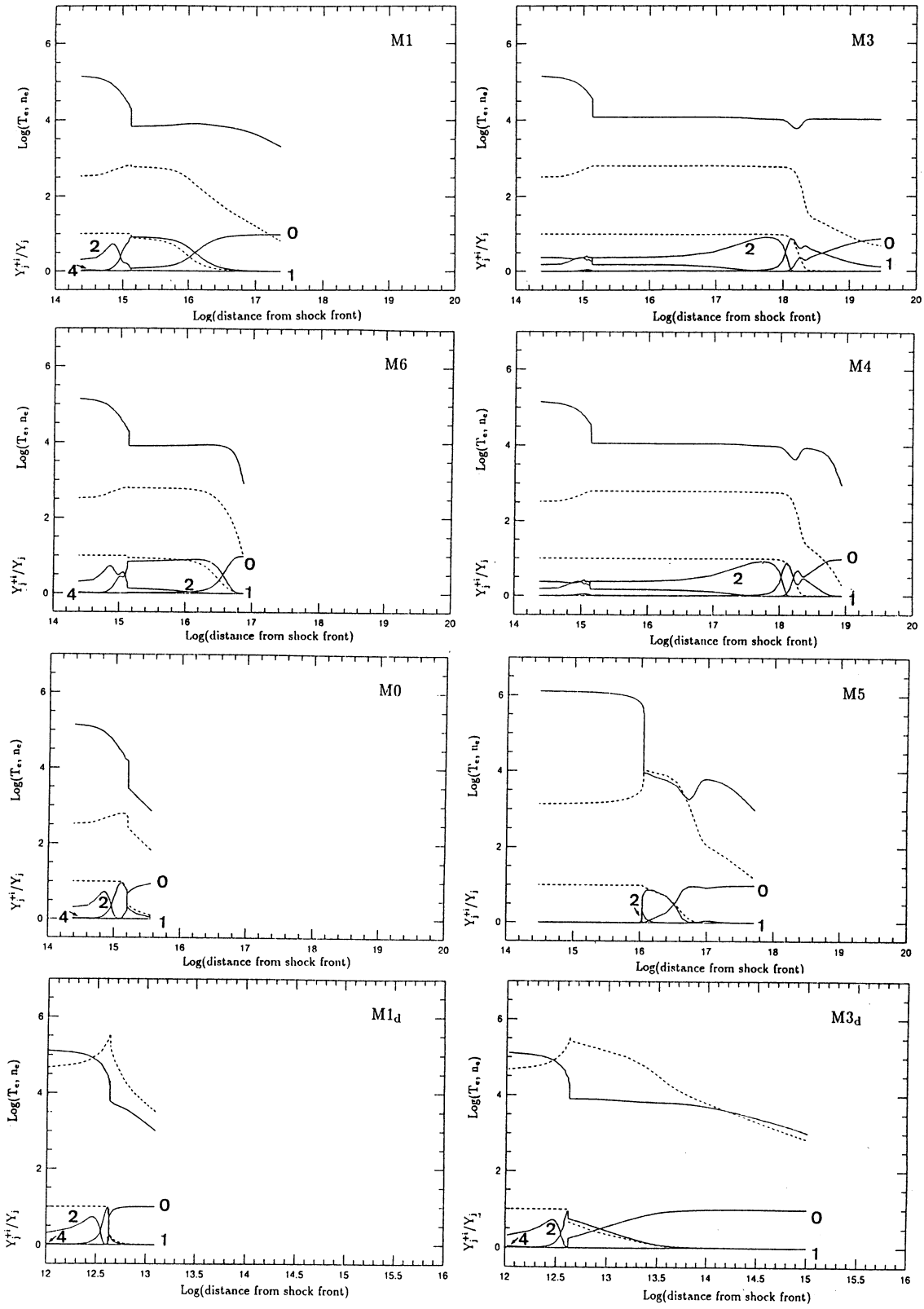

Fig. 1. Top region: the electron temperature (solid lines) and the electron density (dashed lines) across a cloud as functions of the distance from the shock front (in cm). The models represented in the diagrams refer to Table 1. In the bottom of the figures the fractional abundances Y_j^i/Y_j for Ne^{+4}/Ne, O^{+2}/O, N^{+1}/N, N^{+0}/N ions (solid lines), and for H^+/H (dashed line) are given. Numbers near the lines refer to the ions; 0: N^{+0}, 1: N^{+1}, 2: O^{+2}, 4: Ne^{+4}

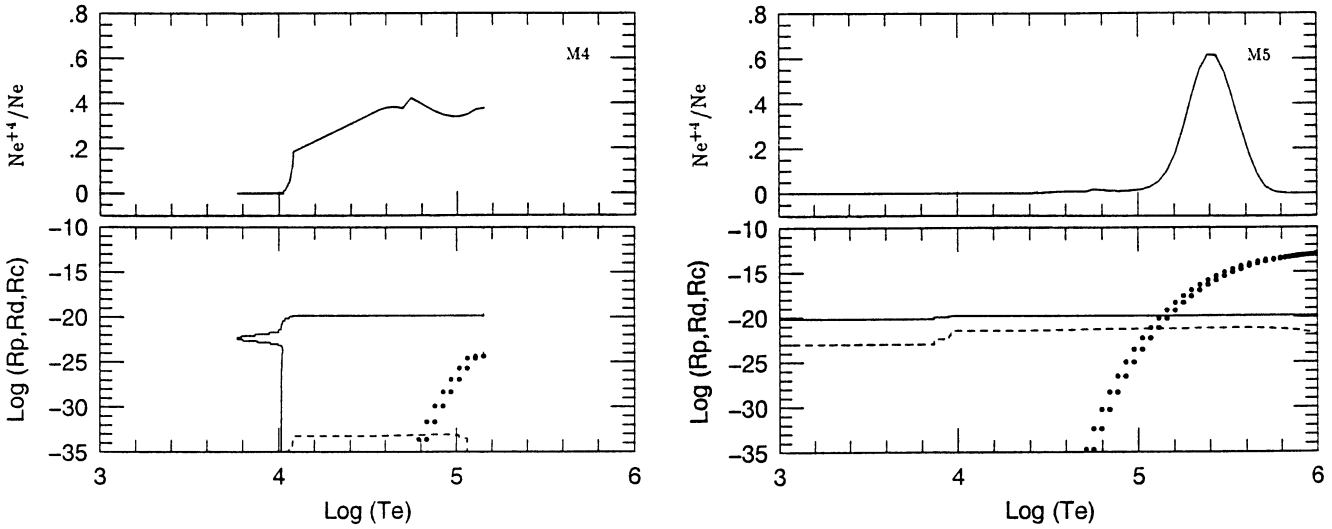

Fig. 2a and b. The ionization rates of the Ne^{+4} ion versus the temperature of the emitting gas for different models (cf Table 1) Ionization by the primary radiation is indicated by solid lines. Ionization by secondary radiation is indicated by dashed lines. Collisional ionization is indicated by dots. In the top of each figure the profile of the fractional abundance of the ion is given **a** M4; **b** M5

low ionization and neutral lines depends on diffuse (secondary) radiation.

Most of the prominent optical - near infrared lines in a Liner spectrum are forbidden. The intensity of a line depends on the fractional abundance of the corresponding ion, on the relative abundance of the element, on the collision strength and statistical weight of the level and term (Osterbrock 1974), and on the volume and density of the gas in the suitable physical conditions. In particular, the fractional abundance of a ion is determined by the ionization rates: the photoionization rate due to radiation from either the AC or the SB (primary radiation), the ionization rate due to diffuse radiation (secondary radiation), and the collisional ionization rate.

In this section we would like to explain concisely the role of the different ionization mechanisms in the line strengths. Some of the most indicative lines are chosen to represent the spectra. These are [Ne V] 3426 which represents the lines from higher levels, [O III] 5007 which is a line from an intermediate ionization level very sensitive to the radiation flux, and [N II] 6583 and [N I] 5200, which represent low ionization and neutral lines, respectively, and are generally strong in the observed spectra of Liners.

3.1. The ionization rates

To understand the line ratios we must know how the fractional abundances of the ions depend in different proportion on the different ionization rates. The ionization rates of Ne^{+4}, O^{+2}, N^{+1}, and N^{+0} as functions of the temperature of the gas are compared in Figs. 2–5, respectively, for different models. R_P is the photoionization rate by the primary radiation (solid lines). R_D is the ionization rate by secondary radiation (dashed lines), and R_C is the collisional ionization rate (dots). The most indicative models are chosen from those presented in Table 1.

Figures 2–5 show that R_P, R_D, and $R_C$are not simple functions of T_e. R_P depends on the optical depth from the surface of the cloud. The diffuse ionizing radiation emitted by the gas is created almost entirely by the recapture of electrons by H and He. R_D depends on the source function of each slab, $S_\nu = j_\nu/k_\nu$ (where j_ν and k_ν are the emission and absorption coefficients, respectively), and on the optical thickness of the slabs (Williams 1967). Collisional ionization rate depends strongly on the temperature of the gas ($\propto T_e^{1/2} \exp(-I'_{Zz}/K\ T_e)$, where I'_{Zz} is the effective ionization potential of the species, and Z and z the ion and the level, respectively (Cox & Tucker 1969). Collisional ionization drops for $T_e \leq 2 \times 10^4$ K. Then, the shock affects mostly the collisional processes which are strongly dependent on the temperature of the gas. Photoionization affects radiative processes and heats the gas to a maximum $T_e \simeq 2 \times 10^4$ K. Therefore, collisional ionization in a pure photoionization model will be insignificant. In the top region of each figure the profile of the fractional abundance of the ion as function of the temperature of the gas is also given.

$R_P$and $R_D$depend on the optical thickness of the gas, therefore, they decrease monotonically with the distance from the shock front.

Figures 2a and 2b show that [Ne V] line can be strong due to both pl photoionization (which prevails on a low V_s shock) and/or pl photoionization accompanied by a relatively strong shock. However, in a radiation dominated condition (model M4) a large fraction of the Ne^{+4} ion is present in gas with $T_e \leq 10^5$ K and is mainly due to the power-law (primary) radiation (Fig. 2a), while at high V_s , represented by model M5, Ne^{+4} is created by collisional ionization at $T_e \geq 10^5$ K (Fig. 2b). In Figs. 3a and 3b the contribution of the different ionization rates to O^{+2} are compared for models representing pl photoionization on a high density gas ($M3_d$) and pl photoionization accompanied by a relatively strong shock (M5), respectively. It can be noticed that

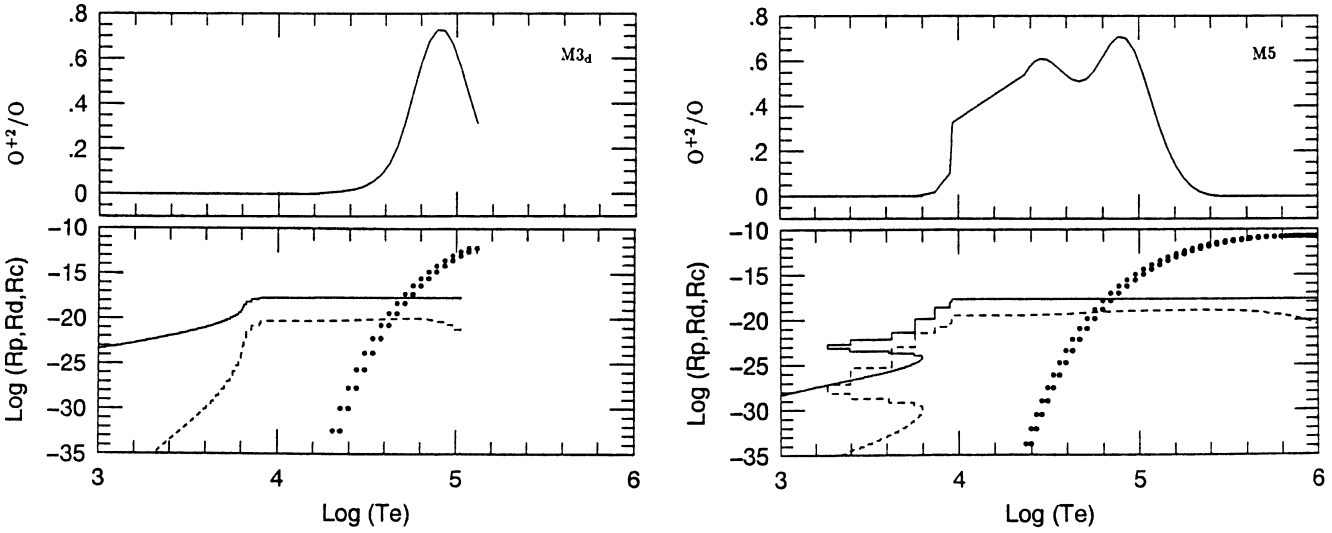

Fig. 3a and b. Same as for Fig. 1 for O^{+2}. **a** $M3_d$; **b** M5

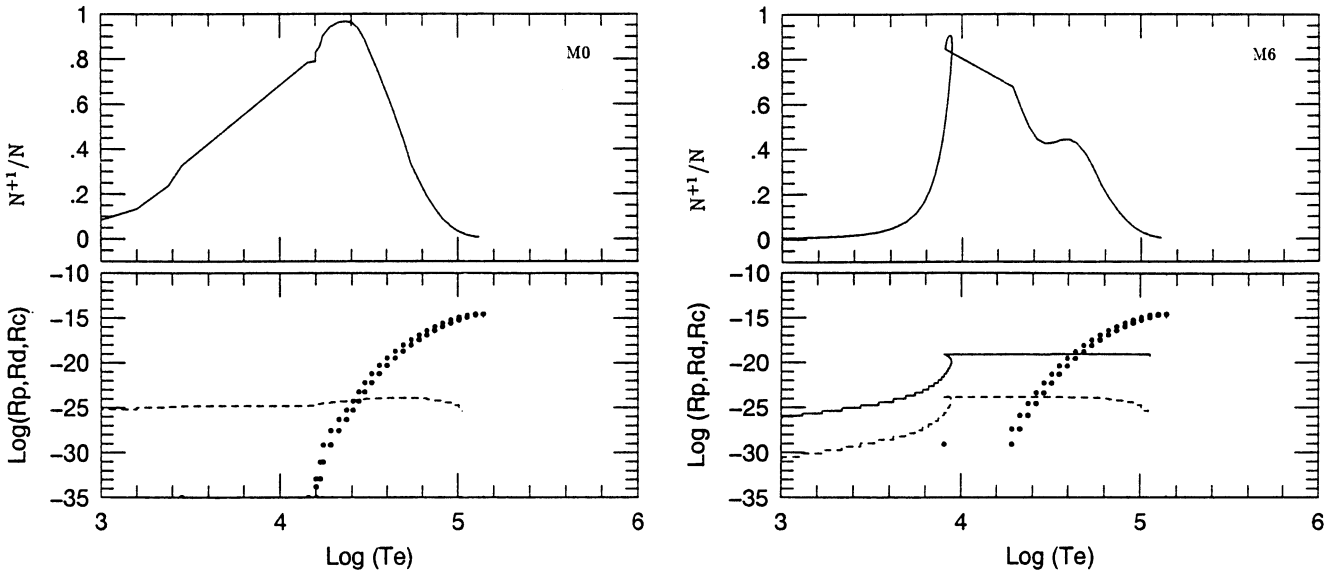

Fig. 4a and b. Same as for Fig. 2 for N^{+1}. **a** M0; **b** M6

in the high density case [O III] lines are emitted from gas at rather high temperatures and are strong due to collisional ionization (Fig. 3a). Figure 3b shows that at lower densities O^{+2} is largely present also at lower temperatures where photoionization is the main cause of ionization. In Figs. 4a and 4b a shock dominated model for low V_s (M0) is compared with a model (M6) where a bb photoionizing radiation is accompanied by the same low shock velocity. Low ionization lines are considered. In a shock dominated case (Fig. 4a) diffuse radiation maintains the gas singly ionized for $T_e \leq 2.5\ 10^4$ K. On the other hand, [N II] lines are emitted by gas at lower temperatures ($\simeq 10^4$ K) and the primary radiation prevails for models dominated by black body radiation with $U \geq 10^{-3}$ (Fig. 4b). Figures 5a and 5b show the different contribution of the ionization rates to the neutral line strength when composite models are characterized by a different V_s (M3 and M5). While diffuse radiation competes with a rather high power-law (primary) radiation to create a strong [N I] (Fig. 5a), strong neutral lines are created mostly by diffuse radiation when compression is strong (Fig. 5b). In this case the optical depth of the gas downstream is high and the primary radiation decreases rapidly with distance from the shock front.

3.2. Calculated line ratios

On the basis of the previous analysis of the ionization rates and conditions downstream it is now possible to understand the line ratios.

It can be noticed that a strong Hβ flux at high F or U requires a large volume of emitting gas in suitable physical conditions (cf Fig. 1 M3, M4, M5). Strong Hβ at high V_s depends on the high

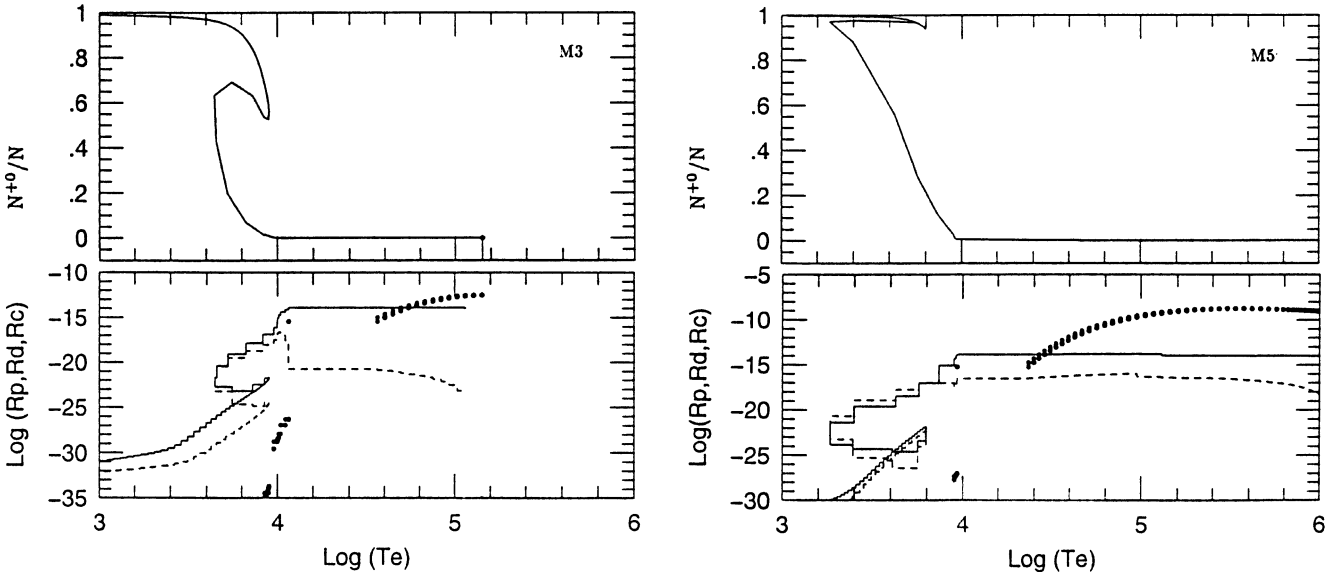

Fig. 5a and b. Same as for Fig. 2 for N^{+0}. **a** M3; **b** M5

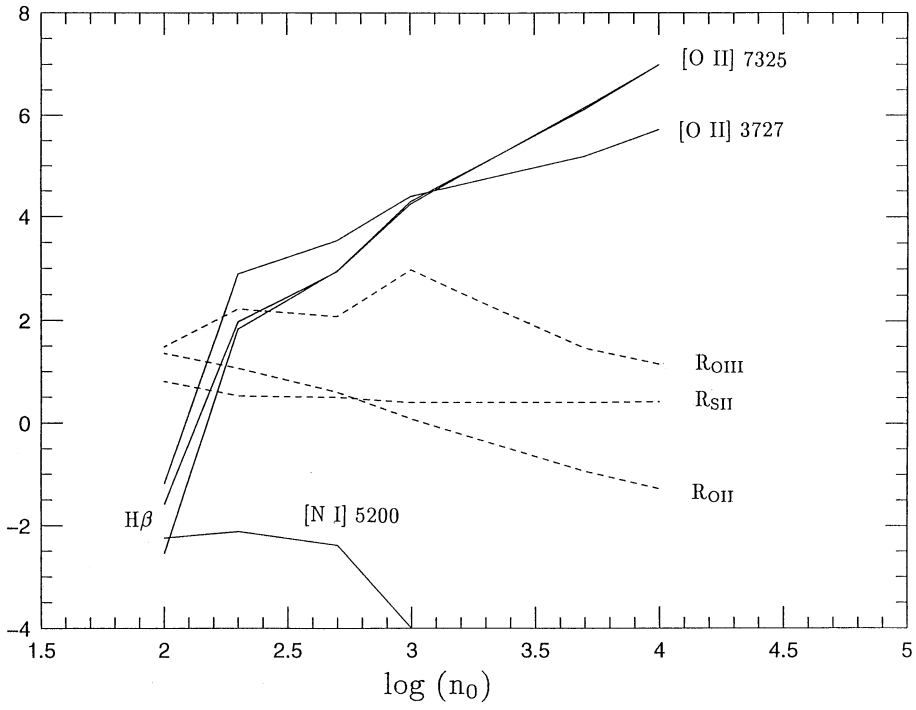

Fig. 6. Log(Hβ), log([O II] 3727+), log([O II] 7325), log([N I] 5200+) (solid lines), and log($R_{[O\,II]}$), log($R_{[O\,III]}$), and $R_{[S\,II]}$(dashed lines) as functions of the preshock density, n_0

density of the emitting gas in the recombination zone (Fig. 1 M5). However, in the high density radiation dominated cases, $M1_d$ and $M3_d$, Hβ is not particularly strong, because the ionized zone throughout the cloud is very small compared to the ionized zone in the low density cases, M1 and M3. In fact, the cooling rate of the gas increases strongly with the density. Figures 1 M1, M3, $M1_d$, $M3_d$ show that $D(M1)/D(M1_d) \simeq D(M3)/D(M3_d) \simeq 10^4 \simeq (n_e(M1_d, M3_d)/n_e(M1, M3))^2$, where D is the geometrical thickness of the ionized zone. In this zone the density $n \simeq n_e$. The high energy cutoff (M4) is not significant in determining the Hβ strength.

[Ne V]/Hβ is high when the shock prevails (M0 and M5) and for high F in case of a power-law. However, notice that the flux of [Ne V] is very low for M0 because Hβ is weak.

[O III] 5007/Hβ increases with F at low densities, due to the high contribution of photoionization. At higher n_0 the contrary is true because the stratification of the ions is different.

$R_{[O\,III]}(\equiv$ [O III] 5007/[O III] 4363) is higher the higher F or U, while the cutoff is not significant. In a shock dominated case (M0) $R_{[O\,III]}$is very low, as in SNR. For M5, in which the effect of the shock and of radiation are comparable, $R_{[O\,III]}$ is similar to that observed for intermediate Seyfert galaxies (Con-

tini & Aldrovandi 1986). Moreover, $R_{[O\,III]}$is very low at high n_0 ($M1_d$ and $M3_d$) because both the density ($\simeq 10^5$ cm^{-3}) and the temperature ($\leq 10^5$ K) of the gas which emits the [O III] lines are relatively high (Fig. 1).

When Hβ is strong, [O II] lines should be strong due to charge exchange reaction, however, [O II] lines are weakened by collisional deexcitation whose critical density are $\simeq$ 3000 cm^{-3}. The calculated $R_{[O\,II]}(\equiv$ [O II] 3727+ /[O II] 7325) are within the range of the observed values (cf the next section), except for M0 and the high density models, $M1_d$ and $M3_d$.

Lines corresponding to singly ionized ions ([N II], [O II], [S II], etc.) and neutral lines ([N I], [O I]) are very sensitive to the cutoff (M4). In fact, the comparison of M3 with M4 in Fig. 1 shows that the X-ray tail of radiation maintains a large region of gas at $T_e \geq 10^4$ K. The [N II]/[N I] ratio is high for $M1_d$ because [N I] is particularly low due to collisional deexcitation. In this case [N I] is mainly due to diffuse radiation. However, [N II]/[N I] is much lower for model $M3_d$ because a strong flux maintains the gas ionized also in the region where $n_e$decreases.

HeII/HeI which depends on radiative recombination of the He lines increases with F. In fact, the line ratio is < 1 for all models except M2, M3, and M4 (cf. Table 1).

4. The high density gas

An important argument regarding Liner spectra concerns the density of the emitting gas. The $R_{[O\,III]}$ratio is generally low indicating high temperatures ($> 10^5$ K) and/or high densities ($> 10^5$ cm^{-3}) in the emitting gas. An accurate study of $R_{[O\,III]}$in AGN is given by Contini & Aldrovandi (1986). High densities, however, are not always compatible with the relatively high $R_{[S\,II]}(\equiv$ [S II] 6717/[S II] 6731) observed line ratios (Sect. 3.2).

It has been suggested that a series of clouds with different densities and velocities characterizes the NLR of Seyfert galaxies, and the gradient of densities follows the gradient of velocities. In particular, lines from the same species (e.g. [O II] 3727 and [O II] 7322) receive different relative contributions from various clouds with different densities and velocities (Filippenko 1985, and Filippenko & Halpern 1984). Therefore, models which include many clouds with different densities were adopted by Viegas-Aldrovandi & Gruenwald (1988, 1990). However, as pointed out in these papers, an additional source of energy is still necessary as, for example, the shock. Moreover, shocked gas shows a large range of densities downstream.

Let us now consider the contribution to the spectrum of lines emitted by high density gas. The observations show that $R_{[S\,II]}$ is generally > 0.8 (Ho et al. 1993) indicating that gas densities are rather low ($\leq 10^3$ cm^{-3}). Also, $R_{[O\,II]}$ is mostly between 5 and 100. In Fig. 6 the calculated line intensities of Hβ, [O II] 3727+, [O II] 7325, and [N I] 5200+ (solid lines), and the calculated line intensity ratios, $R_{[O\,III]}$, $R_{[O\,II]}$, and $R_{[S\,II]}$ (dashed lines), are given as function of n_0. F = 3 10^9 (U = 5 10^{-6}), V_s = 300 km s^{-1}, and $B_0 = 10^{-4}$ gauss are adopted. A model considering the outward motion of the clouds is used for these calculations in order to give results more suitable to the observations.

It can be noticed that the flux of Hβ and of the [O II] lines increases by more than two orders for $n_0 > 10^4$ cm^{-3} which corresponds to a downstream $n \geq 10^6$ cm^{-3}. Line intensities increase with n^2, however, the increase of [O II] 3727 is less straight due to collisional deexcitation and [N I] 5200 decreases strongly at higher densities because the critical density for collisional deexcitation is very low (1.3×10^3 cm^{-3}). Then, if clouds characterized by high densities ($\geq 10^6$ cm^{-3}) contribute to the spectrum, their contribution dominates, i. e. all the line ratios should be characteristic of high densities. Particularly, [N I] should be too weak to be observable. This is not consistent with the observed spectra, because [N I] is high enough in nearly all of them. Moreover, $R_{[S\,II]}$ and $R_{[O\,II]}$ should be lower than 0.5 and 2, respectively. None of the objects included in the sample satisfy all of these conditions.

In conclusion, spectra showing the contributions of both low and high density clouds are realistic, if the relative contribution of very dense clouds is about 10^{-3} times lower than that of low density clouds. It can be estimated that the geometrical thickness of the dense cloud region is smaller than that of NLR clouds by about three orders of magnitude and that dense clouds are located in the innermost zone of the NLR, toward the BLR.

5. Liner spectra

5.1. The individual spectra

We compare now the observational data with calculated spectra for individual objects. A first rough information about the physical conditions of single Liners is obtained by comparing the observational data with the results presented in Table 1 and with diagnostic diagrams (see Appendix). However, not all the spectra can be compared with these results because only some significant models are included. Then, the set of physical conditions which correspond to the best fit of the spectra is calculated for each object.

In Table 2 a–f we present the best fit to the data, within the errors, obtained by composite models. The line intensity ratios to Hβ by Ho et al. (1993) are given and compared with the results of model calculations for each individual object. The calculated Hβ absolute values (at the emitting nebula) are also given. The set of the input parameters which provides the best fit to the observed data appears in the last rows of Tables 2. F and the corresponding ionization parameter U are both given.

Generally, the ratios between lines of the same element depend on the physical conditions of the gas, whereas the fit of line ratios to Hβ depends also on the abundances of the elements relative to hydrogen. The abundance of an element is adjusted when all the corresponding lines show the same trend. However, the intensities of the oxygen lines depend strongly on the physical conditions and oxygen is also a strong coolant, therefore, the stratification of the ionic fractional abundances downstream is modified by changing the O/H relative abundance, which also change the line intensities. Therefore, oxygen line ratios to Hβ are not good measures of the O/H relative abundance. The abundances of some elements (C, Si, S, Fe, etc.) are indicative of dust;

other (C, N, O, etc.) are connected with the type of stars. Argon's single line is usually weak, and, as argon is not a strong coolant, the relative abundance to H can be directly obtained by fitting the calculated to the observed value. Iron lines will be discussed in a forthcoming paper.

For some objects more than one model are indicated. As already mentioned, different types of models fit the observations equally, showing that more observations in different frequency ranges are essential in order to distinguish between the Seyfert and SB phenomena. On the other hand, the $R_{[O\ II]}$and $R_{[O\ III]}$line intensity ratios, which depend on the density and on the temperature of the emitting gas, are not always fitted by single models. Therefore, the contribution to the spectra of clouds in different conditions is considered.

5.2. Discussion

NGC 315 is a Fanaroff Riley type I low luminousity radio galaxy (Venturi et al. 1993), whose optical counterpart is the 12th magnitude dusty elliptical galaxy NGC 315. The observed spectrum (Table 2a) has rather few lines. It is fitted well enough by a low velocity (100 km s^{-1}) shock, low density gas (n_0 = 100 cm^{-3}) and bb radiation, with a rather low ionization parameter U and T_* = 10^5K. NGC 315 most probably is an AGN due to broad Hα emission and the presence of radio jets, however, model results suggest that clouds photoionized by bb radiation dominate the spectrum. Very hot stars and very hot condensation can be present in AGN (see Sect. 1). N/H and Ne/H are about 1.5 times the cosmic values whereas S/H is half. This is consistent with S depletion due to inclusion into dust grains. The contribution to the spectrum from high density regions is excluded because [O II] 3727/Hβ is relatively high.

NGC 404 is classified as a Liner by Ho et al. (1993). The best fit is obtained by low V_s and low n_0, which leads to [S II] 6716/[S II] 6731 $>$ 1 (Table 2a). N/H and S/H are half cosmic, while Ar/H is approximately twice cosmic. A power law spectrum characterized by a rather low F (10^9), corresponding to U = 1.7 10^{-4}, confirms that this Liner contains a low luminosity AGN. The UV source is surrounded by several point sources 3-5 mag fainter (Maoz et al 1995). It is suggested by Maoz et al (1995) that the low- ionization nuclear emission comes from the bright unresolved source, while the strong young stellar features come from the surrounding structure. In fact, a contribution to the spectrum by stars with T_* = 5 10^4 K and U = 10^{-3} may improve the fit to the observations. Notice that the relative abundances are slightly different indicating that the star contribution comes from a different region.

NGC 1052 is a prototype Liner, which shows a complex structure. It was explained as an o.s. (only shock model with F = 0) type by Heckman (1980) on the basis of model calculations which fit SNR conditions rather than those of Liners or AGN. We definitively find that the ionizing radiation is a pl with low F (3 10^9) corresponding to U (5 10^{-4}), and cosmic relative abundances (cf. Viegas & Contini 1994, Fig. 7c). A discrepant value between the calculated and observed [O II] 3727+/[O II] 7325 and [N I]/Hβ ratios, show that regions with different conditions are present and contribute to the spectrum. The observed $R_{[O\ II]}>$ 2 excludes very high densities, however, a model characterized by n_0 = 400 cm^{-3}, V_s = 200 km $s^{-1}$and F=7 10^{10} (U=3.2 10^{-3}) improves the fit. In this model the geometrical thickness of the cloud is reduced to 1 pc. Therefore, the emission from clouds from the inner NLR region, characterized by higher V_s , n_0, and F, is revealed by the line ratios.

NGC 1167 is also classified as a Liner. Our results show that pl radiation with F=3 10^9, corresponding to U = 5 10^{-4}, characterizes the line ratios. V_s (170 km s^{-1}), slightly higher than that calculated for NGC 1052, gives the observed value of [Ne V]. The fit is satisfactory for all lines indicating that the physical conditions of this cloud prevail in the NLR (Table 2b). [N I]/Hβ is twice the observed value; it is, however, acceptable due to the error (50%) of the observational data for weak lines. The result can be improved reducing the geometrical thickness of the cloud. This reduces the low temperature zone where gas is recombined and neutral lines are emitted. N/H is higher than cosmic by a small factor ($<$ 1.5).

NGC 1275 (classified as a Liner by Kirhakos & Phillips 1989) is of intermediate type between Seyfert and BL Lac objects (Böhringer et al. 1993). A radio jet emerges from the nucleus and ends in the radio lobes embedded in the radio halos out to 300 kpc. The emission line complex has two systems with different radial velocities. One is at the velocity of NGC 1275 and a second, centered to NW with recession of 300 km s^{-1} with respect to NGC 1275, is attributed to a spiral galaxy falling into NGC 1275. X-ray emission is observed, as well as the signature of the interaction of the thermal cooling flux plasma with the radio lobes of the galaxy. The best fit of calculated to observed line values is obtained by an only shock (o.s.) model, with rather high V_s and n_0 (Table 2b). This agrees with the formation of a shock due to the interaction of jets with preexisting matter in the outskirts of the galaxy.

A composite model with a flux intensity in agreement with the intensities calculated for Liners (log F = 10 corresponding to U = 6. 10^{-4}, Viegas & Contini 1994, Table 3c) is also well fitting, considering the observational errors.

Dixon et al. (1996) analyzing the far-UV emission with the Hopkins Ultraviolet Telescope found that the O VI/C IV line ratio corresponds to shocks with velocities of 100 - 160 km s^{-1}. They claim that the continuum spectrum of NGC 1275 shows evidence of B-star emission from the high velocity system. Low N/H and S/H indicate the formation of molecular complexes. In fact, the inner regions of this galaxy still contain a considerable amount of molecular gas, which is still forming new stars (Lazareff et al. 1989). However, the results indicate that radiation from the stars is not very important. The shock is strong enough to dominate the very luminous young star clusters formed at the time of the merger. The detection of X-rays is in agreement with the relatively high V_s which is also confirmed by a relatively high [Ne V].

NGC 1667: the spectral line ratios provided by Phillips et al. (1983) are not reddening corrected, therefore it is difficult

Table 3. The summary of results presented in Tables 2

	NGC	type	V_s (km s^{-1})	n_0 cm^{-3}	F	U	T_* (K)	N/H	Ne/H	S/H	flux
1	315	L	100	100	-	1.(-3)	1.(5)	$>$	$\geq$	$<$	bb
2	404	L	100	100	1.(9)	1.8(-4)	-	$<$	c	$<$	pl
			150	100	-	1.(-3)	5.(4)	$<$	c	c	bb
3	1052	L	150	100	3.(9)	5.4(-4)	-	c	c	c	pl
			200	400	7.(10)	3.2(-4)	-	c	c	c	pl
4	1167	L	170	100	3.(9)	5.4(-4)	-	$>$	c	c	pl
5	1275	S	450	200	-	-	-	$<$	$\geq$	$<$	o.s.
			300	300	1.(10)	6.(-4)	-	$<$	$\geq$	$<$	pl
6	1667	S	200	200	4.(10)	3.6(-3)	-	$>$	$>$	c	pl
			500	300	-	-	-	$>$	c	c	o.s.
7	2639	L	100	100	-	1.(-3)	1.2(5)	$>$	c	$<$	bb
			150	100	1.(8)	1.8(-5)	-	$>$	$>$	c	pl
8	2841	L	150	100	-	1.(-2)	7.(4)	$>$	c	c	bb
9	3031	L	200	600	6.(10)	1.8(-3)	-	c	c	c	pl
			200	300	3.(10)	1.8(-3)	-	c	c	c	pl
			100	100	1.(8)	1.8(-5)	-	$>$	c	$>$	pl
10	3504	-	100	100	1.(7)	1.8(-6)	-	$>$	c	$<$	pl
			100	100	-	1.(-2)	5.(4)	$>$	c	$<$	bb
11	3642	-	100	100	-	1.(-2)	8.(4)	$>$	$>$	c	bb
			100	100	3.(7)	5.4(-6)	-	$>$	$>$	$<$	pl
12	3998	-	140	200	-	1.(-2)	1.(5)	c	c	c	bb
			100	100	1.(9)	1.8(-4)	-	c	$>$	$<$	pl
13	4395	S	200	200	1.(11)	9.(-3)	-	$<$	c	c	pl
14	4618	H	150	100	-	1.(-3)	2.(4)	$<$	c	c	bb
			150	100	-	1.(-2)	5.(4)	$<$	$>$	$<$	bb
15	7217	L	100	100	-	1.(-3)	5.(4)	$>$	$>$	$>$	bb
16	7479	L	150	100	1.(8)	1.8(-5)	-	$>$	$>$	c	pl
			150	100	-	1.(-3)	1.(5)	$>$	$>$	c	bb
17	7714	H	150	100	-	1.(-2)	5.(4)	$>$	c	$<$	bb
			300	300	-	1.(-2)	5.(4)	$<$	c	c	bb
18	7743	L	150	100	-	1.(-1)	6.(5)	c	$>$	$<$	bb
			300	200	-	-	-	$>$	$>$	$<$	o.s.

to compare them with those by Ho et al. (1993). Phillips et al. (1983) conclude that *in the majority of Sandage high - excitation galaxies the predominant ionization source is not the radiation of the young hot stars but rather is nonthermal in origin*. We test three possible interpretations of the spectrum. Table 2 b shows that the pl radiation dominated model gives a poor fit, because [Ne V] is nearly absent, and [O II] 3727+/[O I] 6300 ratio is very low relative to the observed one, however, a bb spectrum requires too high a star temperature. The o.s. model included in Table 2b gives a very low [O II] 3727+/[O II] 7325 ratio. A characteristic common to all sets of results is the rather high N/H relative abundance. A FWHM ([O III]) = 290 km s^{-1}, given by Phillips et al. (1983), agrees with the adopted average V_s. We suggest that this galaxy cannot be explained by a unique radiation type. In fact, recent observations by Radovich & Rafanelli (1995) in different location of the galaxy show that different spectra are emitted from the nuclear, off-nuclear, and circumnuclear regions. The fit of the observed line ratios with calculated ratios by pure photoionization models is quite good; however, some indicative lines ([Ne V], [O II] 7325, [S III], etc.) are not included in the observational sample. Moreover, the fit of the [O III] 4363 line is rather poor. We suggest that a better fit could be obtained including the effect of the shock. Particularly, the heating of the emitting gas at higher temperature should improve the fit of the [O III] 4363/[O III] 5007 line ratio.

NGC 2639 is a "classical" case of a Liner which can be equally well fitted by pl and bb radiation. In both cases N/H is > 1.5 cosmic and S/H is rather low. Moreover, U or F are low, confirming the low-luminosity nature of Liners. As already explained in the case of NGC 315, hot gas concentrations and even very hot stars can exist in an AGN without being alternative to the AGN phenomenon.

NGC 2841 is most likely to be a starburst with $T_* = 7 \times 10^4$ K. It is also characterized by a N/H higher than cosmic by a factor of 3 (Table 2c).

NGC 3031 (M81) is an example of Liners in which all lines do not have the same width, as in NGC 3998. FWHM between 2200 ± 200 km s^{-1}and 210 ± 45 km s^{-1}for Hα, and between a maximum of 1090 ± 300 km s^{-1}for [Ne V] and a minimum of

190 ± 45 km s^{-1}for [S II] 6583 are shown by Ho et al. (1996, Table 2). It is also included in the sample of Zaritsky et al. (1994), where the properties of individual H II regions in spiral galaxies are investigated. They deduce O/H relative abundances between 7.76×10^{-4} and 1.25×10^{-3}, with lower values in the outskirts. We have added to the observations by Ho et al (1993) the recent observations by Ho et al. (1996) which are indicated by obs* in Table 2c. A rough fit to the observational data is obtained by adding to the spectrum calculated by the parameters, which fit the Liner definition, other contributions of models with higher densities, velocities and radiation intensities. We obtain roughly cosmic abundances and slightly higher N/H and Ne/H in one case.

Ho et al. (1996) claim that the presence of more than one ionization parameter components in M 81 in the NLR conflicts with the density stratification picture and indicates that the actual NLR structure must be more complicated. On the other hand, a higher ionization parameter accompanied by higher velocities and densities strengthens our previous models for AGN relative to the distribution of the physical parameters in the NLR (cf. Contini & Viegas-Aldrovandi 1991 and Contini 1988).

The observed Hβ flux at earth is 5.4 10^{-14} erg cm^{-2} s^{-1}(Ho et al. 1996) which corresponds to 7 10^{-3} erg cm^{-2} s^{-1}at the emitting nebula, adopting a distance of 3.6 Mpc, and a radius of the emission regions of 10 pc (Ho et al 1996). Comparing with the calculated Hβ flux, a filling factor of ~ 0.04 is deduced.

NGC 3504: its spectrum is a typical example of an average between a pl with very low F and a bb from young stars. This justifies the high N/H ratios relative to cosmic. S/H are lower by a factor of 1.5 - 3, indicating that dust could be present. Velocities and densities are low, as usual in Liners (Table 2d).

NGC 3642: observations of the IR continuum are included in the Willner et al. (1985) Liners sample. We find a bb spectrum in the fitting process (Table 2 d) with rather high T_*; however, some line intensities are too low, compared to the observed values. The contribution from clouds photoionized by pl radiation characterized by a low intensity (log (F) ≥ 7) strongly improves the fit of [O II] 7325 and [S III] 9532 line ratios to Hβ. Ne/H is ~ 3 times higher than the cosmic value, accompanied by a rather high N/H.

NGC 3998: the Hα line profile consists of a narrow core (FWHM ~ 500 km s^{-1}), which provides ~ 25 % of the flux, sitting on broad wings (FWHM ~ 3300 km s^{-1}) (Heckman 1980). This supports the possibility that Liners may have a BLR as do Sy 1 and QSO. A good fit is obtained with $V_s = 140$ km s^{-1} and a bb spectrum with rather high T_* (Table 2d). The contribution of different regions to the spectrum is indicated by the [S II] 4073/[S II] 6716 + ratio, which is lower by a factor of ~ 6 in the model than the observations. In fact, a composite model accounting for a pl radiation flux with log (F) = 9 and lower V_s (100 km s^{-1}) and n_0 (100 cm^{-3}) strongly improves the fit of this line ratio.

NGC 4395: the fit (Table 2 e) is not very satisfactory. A pl spectrum is, however, indicated with rather high F and very low N/H. In fact, a bb type must be discarded on the basis of too low [Ne V]/Hβ, He II/Hβ, and [S III]/[S II] line ratios. This galaxy is classified as Sy 1 (Filippenko & Sargent 1989) on the basis of the broad line components. They claim that the emission line spectrum is similar to that emitted by Sy 2 galaxies or even by Liners. Higher shock velocities and densities than observed in Liners suggest that the spectrum of this galaxy may be similar to that of a Sy 2 or to the spectrum emitted from the NLR of a Sy 1 galaxy. Lines up to very high ionization levels are observed. Particularly, [Fe X] implies temperatures $> 10^6$ K in the emitting gas. These high temperatures correspond to shocks of $V_s \geq 250$ km s^{-1}. The contribution of emission from gas at higher V_s and higher n_0 improves the fit of some important lines such as [O III] 4363. On the other hand, the observations show FWHM of about 60 km s^{-1}. The width of the [Fe X] line can be hardly recognized in the spectrum, nevertheless, the discrepancy between calculated and observed widths can be slightly reconciled considering that the models refer to the FW0M which is generally higher than the FWHM.

NGC 4618: the spectrum characteristic of SB is the result of a mixture of bb with different T_*, U, and B_0, indicating the effect of many different regions (Table 2e). Let us notice, however, that Hβ absolute intensity is much lower at lower T_* and lower U and a weighted mean must be considered. Shock velocities and densities are appropriate to Liners. Nitrogen is less than or about cosmic, whereas S/H is higher or lower than cosmic depending on the model.

NGC 7217 is included in Keel's (1983) sample of normal spiral galaxies with low ionization emission and is also defined as a Liner by Willner et al. (1985). Our results indicate a SB galaxy with higher than cosmic abundances, particularly for N, Ne, and S (Table 2e).

NGC 7479 is classified as a barred galaxy by Telesco et al. (1993) The IRAS colors appear to be intermediate between those of Sy and SB. Nearly 70% of the emission arises in one pixel, so that all of the IR luminosity could be powered by a nonthermal source. The ambiguous nature of this galaxy appears also in Table 2 f. The spectrum can be satisfactorily fitted by both bb and pl radiation and in both cases [O II] 7325 is overestimated by the calculations. In particular, [O II]/Hβ in the pl case is higher than the observed value by a factor 10, probably excluding the model.

NGC 7714: the spectrum is characterized by low [N II], [S II], and [O I] to Hβ line ratios relative to the other galaxies in the sample. French (1980) includes it among the H II galaxies region and indicates (in his Table X) N/H, O/H, and Ne/H relative abundances lower than cosmic by a factor 2 - 3. Weedman et al. (1981) defines this galaxy as a prototype SB with very massive hot stars and explains the X-rays by a high SN rate. We also find a good fit with bb radiation and relatively hot stars (Table 2f). Two different models can be found. One has rather high V_s, high n_0 and a lower N/H abundance ratio. Strong X-rays fluxes result from higher V_s, which supports this case. On the other hand, the N/O = 0.197 which results from the

low V_s model is in better agreement with N/O = 0.148, found by Storchi-Bergmann et al. (1994), than the N/O = 0.03 from the high V_s model. S/O abundance ratios between 0.015 and 0.024 are found by model calculations; they are both in good agreement with S/O = 0.019 found by Storchi-Bergmann et al. (1994).

NGC 7743 shows very strong [O II] 3727 and [O III] 5007 lines accompanied by a relatively low [O I] (ratios to Hβ). Moreover, [Ne III]/Hβ is very high. The only good fit (Table 2 f) is obtained by bb radiation from an extremely hot source. The fit to the O lines can be obtained by an o.s. model with high V_s (300 km s^{-1}), in agreement with Storchi-Bergmann & Pastoriza (1989). However, in this case [Ne V] is very high and [O II] 7325/Hβ is out of the observed range. We have tried to use a pl model, but even with increased O/H and Ne/H relative abundances to fit the high line ratios, no pl model fits the low [O III]/[O II] ratio. Alternative models, characterized by clouds in which the shock front edge is affected by the radiation flux (cf. Sect. 1), do not fit either. Also in this case [Ne V]/Hβ line ratios are extremely high. Moreover, [N I] and [O I] lines are strong enough to exclude 'matter bound' models corresponding to a very small geometrical thickness of the emitting clouds. This discussion illustrates the danger of drawing conclusions based on a small number of spectral lines.

6. Conclusions

In previous sections we have explained the line ratios in Liner spectra considering the different ionization processes. The role of collisional ionization was investigated in particular depth. Model results show that [Ne V] lines can be strong due both to collisional ionization and/or photoionization. Lines from the II and III ionization levels are generally due to photoionization, but a strong contribution by collisional ionization appears in case of high densities and/or of a strong shock. Neutral lines are enhanced by diffuse radiation. The contribution of high density gas to the line intensities in Liners spectra is very small, indicating that the high density region, located between the NLR and the BLR, is also small.

On the basis of diagnostic diagrams it is possible to obtain a first information from Liner observed spectra for single cases.

A summary of the results obtained from numerical simulations by SUMA for individual Liners of the Ho et al. (1993) sample is presented in Table 3. In the first column the numbers refer to diagnostic diagrams (see Appendix). The objects are listed in the second column. Their classification is given in column 3, the shock velocity in column 4, the photoionizing pl radiation flux in column 5, the ionization parameter in column 6, and the star temperature in column 7. In the next three columns qualitative values of relative abundances ratios to the cosmic ones (Allen 1983) are given for N/H, Ne/H, and S/H (>: higher than cosmic, c: cosmic, <: lower than cosmic); O/H is about cosmic for all objects. In the last column the type of the ionizing radiation responsible for heating and ionization of the emitting gas is indicated.

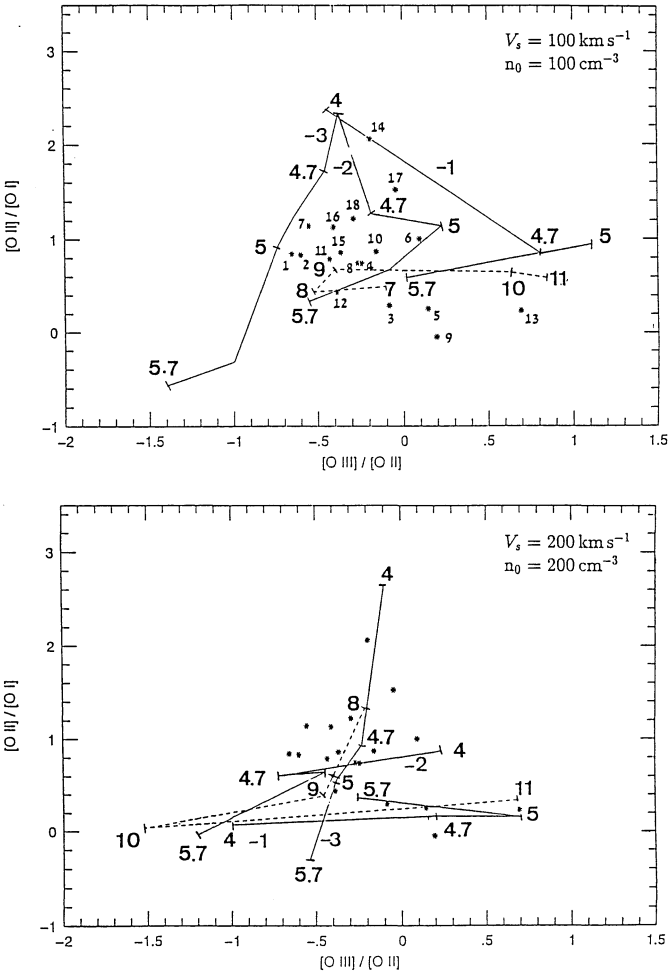

Fig. A1a and b. [O II] 3727+/[O I] 6300+ versus [O III] 5007+/[O II] 3727+. **a** V_s =100 km s^{-1}, n_0=100 cm^{-3}; **b** V_s =200 km s^{-1}, n_0=200 cm^{-3}

In most of the objects a bb source coexists with pl radiation from the AC. Shocks are always present, even if the spectra of many objects are radiation dominated. A maximum density of 500 - 600 cm^{-3} is deduced by the calculations in a few objects and a maximum velocity of 450 -500 km s^{-1}in two of them. F and U are relatively low, as well as V_s and n_0. Furthermore, the best fit of the spectra in the bb radiation dominated case is obtained - as in the pl case - by models implying that the shock front edge of the cloud is opposite to the edge reached by the radiation flux. As the clouds are moving outward, this indicates that the source of radiation (active nucleus or young stars) is located in the central region of the galaxy. For most of the objects included in the sample, the N/H and Ne/H relative abundances are high and S/H slightly low.

It can be noticed that 3 out of 10 L objects (Liners) are of pl type. (NGC 1052, NGC 1167, and NGC 3031). They can be considered as AGN characterized by a low F, low V_s and low n_0. Regarding the other L galaxies, in 3 of them radiation from a bb source prevails (NGC 315, NGC 2841, and NGC 7217) with $T_* \sim 5 \times 10^4$ K, showing SB characteristics: $V_s <$

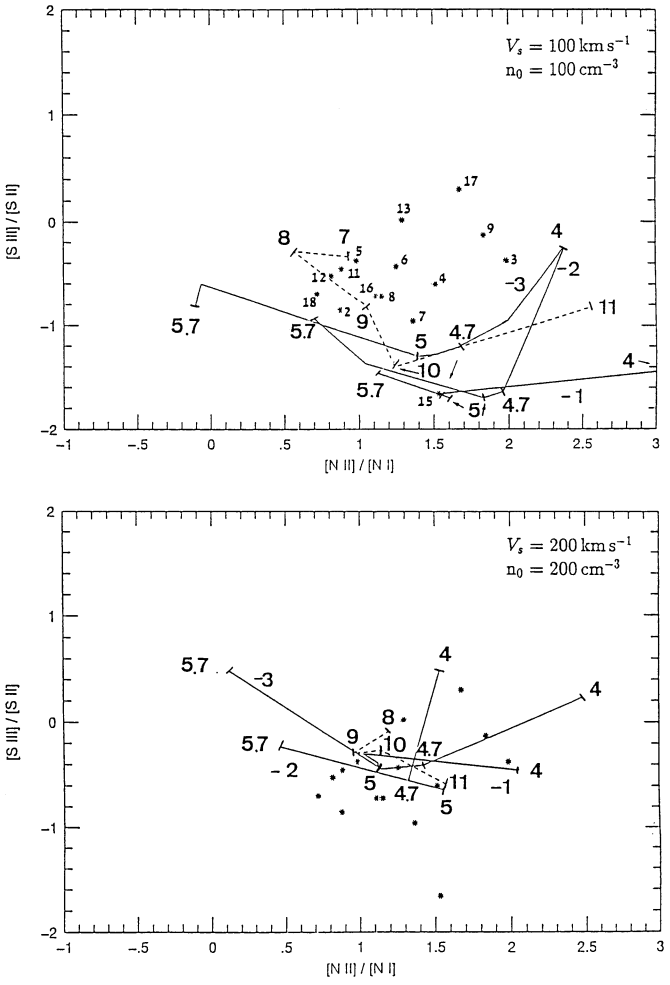

Fig. A2a and b. [S III] 9532+/[S II] 6716+ versus [N II] 6548+/[N I] 5200+. **a** V_s =100 km s^{-1}, n_0=100 cm^{-3}; **b** V_s =200 km s^{-1}, n_0=200 cm^{-3}

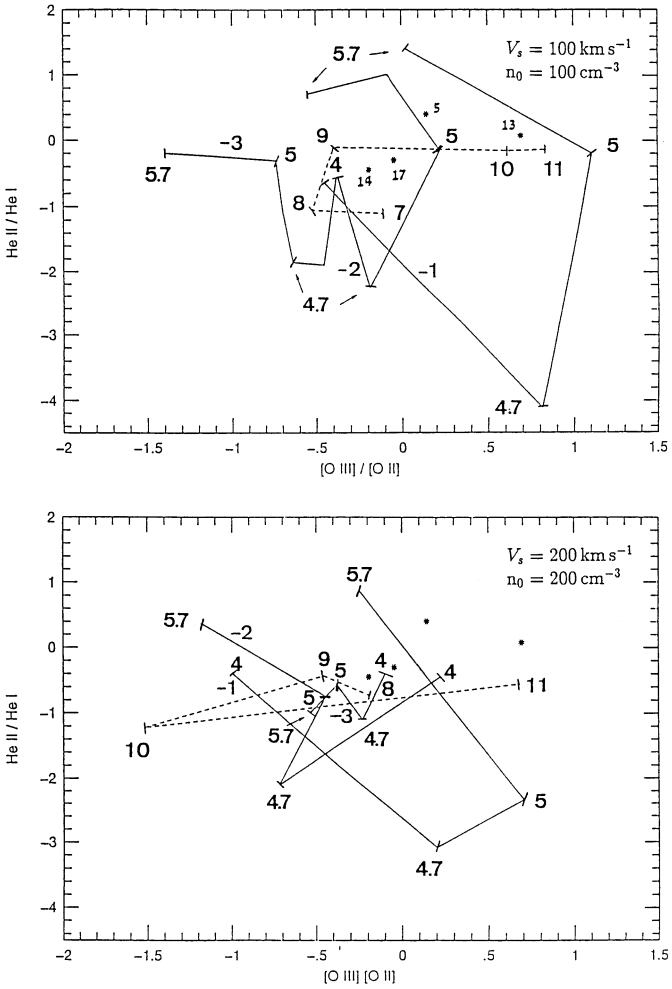

Fig. A3a and b. He II 4686/He I 5876 versus [O III] 5007+/[O II] 3727+. **a** V_s =100 km s^{-1}, n_0=100 cm^{-3}; **b** V_s =200 km s^{-1}, n_0=200 cm^{-3}

250 kms^{-1}, higher than cosmic N/H, higher or normal Ne/H, and mostly lower S/H, which indicates the presence of dust. The other ones (NGC 404, NGC 2639, and NGC 7479) show that pl and bb photoionization are both effective. The exceptionally high [O I]/Hβ ratio observed in the spectrum of NGC 3031 is characteristic of rather high V_s , n_0, and T_*. The other object classified as Liner, NGC 7743, is ambiguous.

The three S objects (Seyfert), NGC 1275, NGC 1667, and NGC 4395, show pl radiation dominated spectra with a strong contribution from shocks with relatively high V_s and F. Interestingly, the observed [Ne V]/Hβ is rather high for these objects: 0.91, 0.97, and 0.86 for NGC 1275, NGC 1667, and NGC 4395, respectively. They are characteristic of higher V_s and n_0, which fit Seyfert 2 galaxies rather than Liners and do not appear in the sample of models presented in Table 1.

The two H objects (H II), NGC 4618 and NGC 7714 show bb radiation with U ($\leq 10^{-2}$) and $T_* \leq 5 \times 10^4$ K.

As for the 3 objects which do not appear in Table 1 of Ho et al. (1993), NGC 3504, NGC 3642, and NGC 3998 show mixed characteristics of low luminosity Seyfert 2 galaxy and SB.

In conclusion, in previous sections we have given the physical conditions in single Liners using calculations by composite models. We have shown that shocks and a photoionizing flux are usually present with comparable importance. Indeed, uncertainties due to model simulations and observational errors must be considered. The different spectra of Seyfert type and SB galaxies are confirmed, however, in many AGN, clouds ionized by the power-law radiation from the active center coexist with clouds ionized by black body radiation from stars and/or hot condensations. Some objects still need more sophisticated models in order to be better understood. This will be done in future works on individual galaxies.

Acknowledgements. I am very grateful to the Referee, Dr. Ho, for enlightening remarks.

Appendix: diagnostic diagrams

In Figs. A1–A4 we present the results of model calculations and we compare them with the observational data of the present sample. Nevertheless, the diagrams can be used as a basis for the

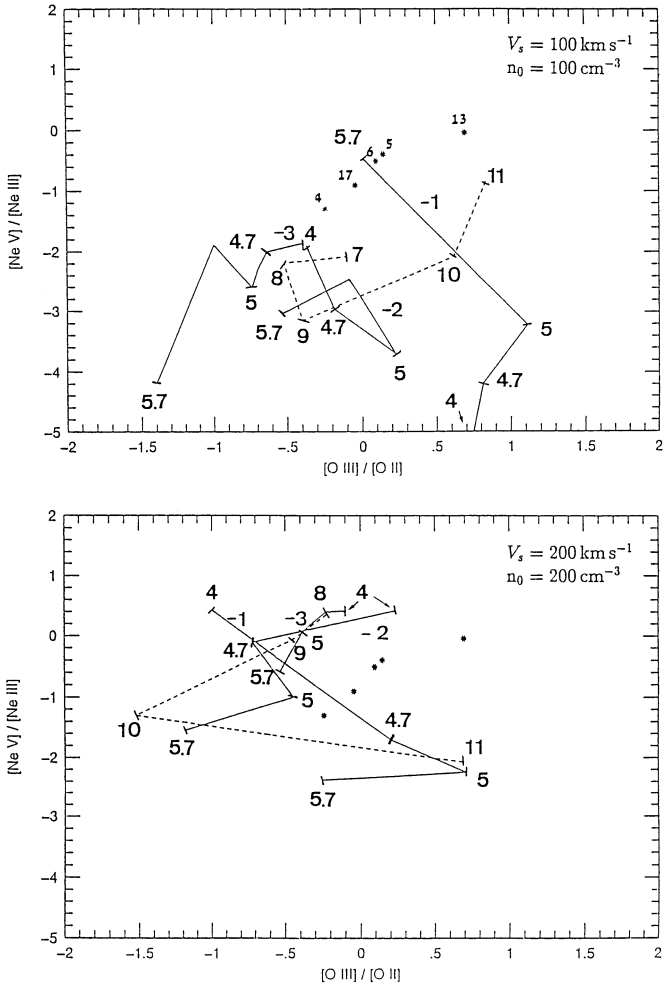

Fig. A4a and b. [Ne V] 3426+/[Ne III] 3869+ versus [O III] 5007+/[O II] 3727+. **a** V_s =100 km s^{-1}, n_0=100 cm^{-3}; **b** V_s =200 km s^{-1}, n_0=200 cm^{-3}

interpretation of any spectrum. The most indicative line ratios of single elements in different ionization stages are considered in order to avoid the problem of relative abundances. Cosmic abundances (Allen 1983) and $B_0 = 10^{-4}$ gauss are used in the calculations.

In Figs. A1 [O II] 3727+/[O I] 6300+ versus [O III] 5007+/[O II] 3727+ is given (+ indicates that the doublet is considered). In Figs. A2 [S III] 9532+/[S II] 6716+ versus [N II] 6548+/[N I] 5200+ appears, followed by He II 4686/He I 5876 versus [O III] 5007+/[O II] 3727+ in Figs. A3. Finally, [Ne V] 3426+/[Ne III 3869+ versus [O III] 5007+/[O II] 3727+ appears in Figs. A4. In each figure two diagrams are given, depending on the shock velocity and on the preshock density. These parameters are chosen in order to fit the conditions which prevail in the NLR clouds; therefore, higher densities correspond to higher velocities.

On the top right side of each diagram V_s and n_0 are indicated. Solid lines refer to composite models which are calculated adopting bb radiation; they are marked by the value of log (U). The tags indicate the corresponding log (T_s). Dashed lines refer to composite models calculated adopting a pl radiation; the values of log (F) are indicated by the tags. Small numbers near the asterisks, representing the observational data of single objects, are given in Table 3. They appear only in one diagrams of each figure in order to permit a clear view in the next diagram.

Figures A1–A4 show that the ranges of model results calculated in the pl case and those calculated in the bb case coincide in most of the diagrams. This explains the ambiguity of Liners as objects which could belong to either the AGN or SB phenomena. Moreover, some data are better fitted by models with low V_s , other by relatively high V_s ; this indicates that the shock plays an important role in Liners.

References

Allen, C. W. 1983, in 'Astrophysical Quantities', The Athlone Press, p. 30
Baldwin, J. A. et al 1996, ApJ, 461, 664
Balik, B., Heckman, T. 1985, AJ 90, 197
Böhringer, H., Voges, W., Fabian, A. C., Edge, A. C., Neumann, D. M. 1993, MNRAS 264, L25,
Contini, M. 1988 ApJ, 333, 181
Contini, M., Aldrovandi, S. M. V. 1983, A&A 127, 15
Contini, M., Aldrovandi, S. M. V. 1986, A&A 168, 41
Contini, M., Viegas, S. M. 1991, ApJ 373, 405
Contini, M., Viegas, S. M. 1992, ApJ 401, 481
Contini, M., Viegas - Aldrovandi, S. M. 1989, ApJ 343, 78
Contini, M., Viegas - Aldrovandi, S. M. 1990, ApJ 350, 125
Contini, M., Prieto, M. A., Viegas, S. M. 1995, MNRAS submitted
Cox, D. P., Tucker, W. H. 1969, ApJ 157, 1157
Dahari, O., De Robertis, R. R. 1988, ApJS 67, 249
Diaz, A. I., Pagel. B. E. J., Wilson, R. G. 1985, MNRAS 212, 737
Dixon, W. V-D., Davidsen, A.F., Ferguson, H.C. 1996, AJ 111, 130
Dopita, M.A., Sutherland, R.S. 1995, ApJ 455, 468
Dopita, M.A., Sutherland, R.S. 1996, ApJS 102, 161
Filippenko, A. V. 1985, ApJ 289, 475
Filippenko, A. V., Halpern, J. P. 1984, ApJ 285, 458
Filippenko, A. V., Sargent, W. L. W. 1985, ApJS 57, 503
Filippenko, A. V., Sargent, W. L. W. 1989, ApJ 342, L11
French, H. B. 1980, ApJ 240, 41
Heckman, T. M. 1980, A&A 87,152
Ho, L. C., Filippenko, A. V., Sargent, W. L. W. 1993, ApJ 417, 63
Ho, L. C., Filippenko, A. V., Sargent, W. L. W. 1996, ApJ 462, 183
Keel, W. C. 1983, ApJ 269, 466
Kirhakos, S., Phillips, M. M. 1989, PASP 101, 949
Lazareff, B., Castets, A., Kim, D.-W., Jura, M. 1989, ApJ 336, L13
Lipari, S., Terlevich, R., Macchetto, F. 1993, ApJ 406, 451
Lonsdale, C. J., Lonsdale, C. J., Smith, H. E. 1992, ApJ 391, 629
Maoz, D. et al. 1995, ApJ, 440, 91
Morse, J.A., Raymond, J.C., Wilson, A.S. 1996, PASP, 108, 426
Osterbrock, D. E. 1974 in Astrophysics of Gaseous Nebulae, ed. W. H. Freeman and Company, San Francisco.
Osterbrock, D. E., Tran, H. D., Veilleux, S. 1992, ApJ 389, 196
Phillips, M. M., Charles, P. A., Baldwin, J. A. 1983, ApJ 266, 485
Radovich, M., Rafanelli, P. 1995, A&A 306, 97
Shuder, J. M., Osterbrock, D. E. 1981, ApJ, 250, 55
Storchi-Bergmann, T., Pastoriza, M. G. 1989, ApJ 347, 195
Storchi-Bergmann, T., Calzetti, D., Kinney, A., L. 1994, ApJ 429, 572
Telesco, C. M., Dressel, L. L., Wolstencroft, R. D. 1993, ApJ 414,120
Terlevich, R., Melnick, J. 1985, MNRAS, 213, 841

Terlevich, R., Tenorio-Tagle, G., Franco, J., Melnick, J. 1992, MNRAS 255, 713
Veilleux, S., Osterbrock, D. E. 1987, ApJS 63, 295
Venturi, T., Giovannini, G., Feretti, L., Comoretto, G., Wherle, A. E. 1993, ApJ 408, 81
Viegas-Aldrovandi, S. M., Gruenwald, R. B. 1988, ApJ 324, 683
Viegas-Aldrovandi, S. M., Gruenwald, R. B. 1988, ApJ 360, 474
Viegas-Aldrovandi, S. M., Contini, M. 1989, ApJ 339, 689
Viegas, S. M., Contini, M. 1994, ApJ 428, 113
Weedman, D. W., Feldman, F. R., Balzano, V. A., Ramsey, L. W., Sramek, R. A., Chi-Chao Wu 1981, ApJ 248, 105
Williams, R. E. 1967, ApJ 147, 556
Willner, S.P., Elvis, M., Fabbiano, G. F., Lawrence, A., Ward, M. J. 1985, ApJ 299 443
Zaritsky, D., Kennicutt, R. C., Huchra, J. P. 1994, ApJ 420, 87